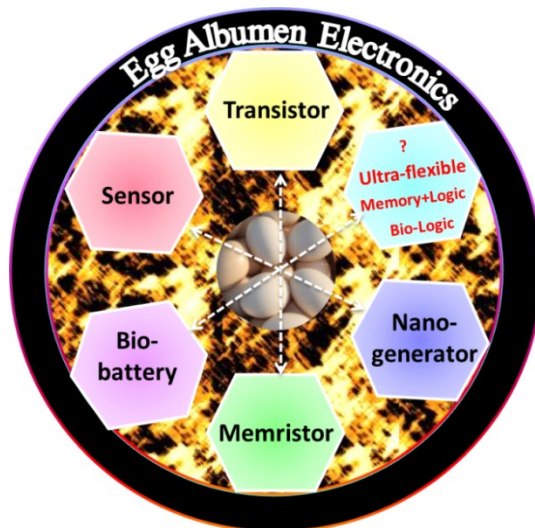


## Supporting Information

### Artificial and wearable albumen protein memristor arrays with integrated memory logic gate functions †

Guangdong Zhou,<sup>a‡</sup> Zhijun Ren,<sup>a‡</sup> Lidan Wang,<sup>a‡</sup> Bai Sun,<sup>b</sup> Shukai Duan<sup>a\*</sup> and Qunliang Song<sup>a\*</sup>



**Fig. S1** Schematic of egg albumen-based electronic devices. The functionalized egg albumen can be served as host-material applied in a variety of electronic devices, but the natural flexible electronic device is absence.

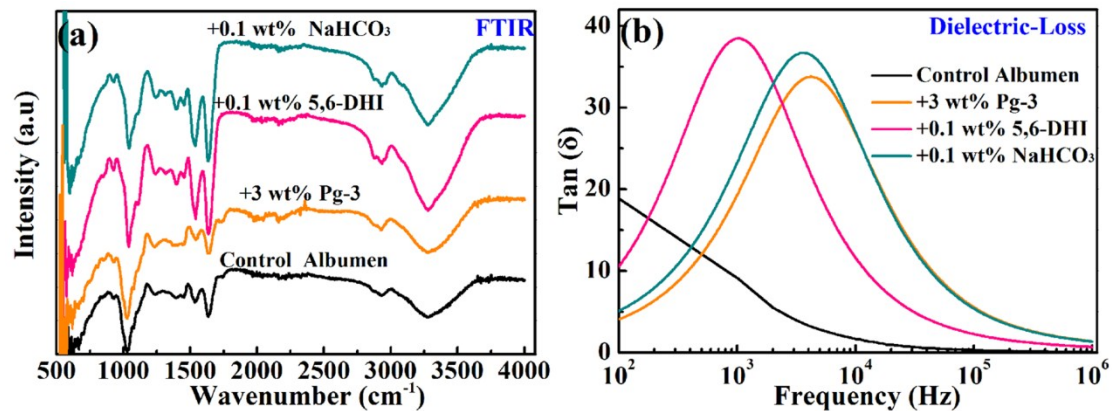


**Fig. S2** (a) Fourier transform infrared spectroscopy spectrum (FTIR) of the fabricated albumen matrixes. (b) Dielectric loss *versus* Frequency curves for the control albumen samples after adding Pg-3, 5, 6-DHI and NaHCO<sub>3</sub>. The permittivity at high and low frequencies shows a very different. At low frequency (<10<sup>2</sup> Hz), the permittivity and frequency dispersion are mainly dominated by space charge polarization, namely, the interface-related polarization is the key factor. Entering into the relative high frequency (1~100 MHz), the permittivity and frequency dispersion are mainly dominated by turn-direction polarization, in other words, the material body-related polarization is the key factor. When entering into the high frequency region (>100 MHz), the ionic-polarization dominates the permittivity, as demonstrated in the above schematic. For the egg albumen, the permittivity @1 MHz was focused. In fact, the great frequency dispersion during 10<sup>3</sup>~10<sup>4</sup> Hz is very interesting phenomenon, it is possibly co-dominated by the interface- and body-related polarization.

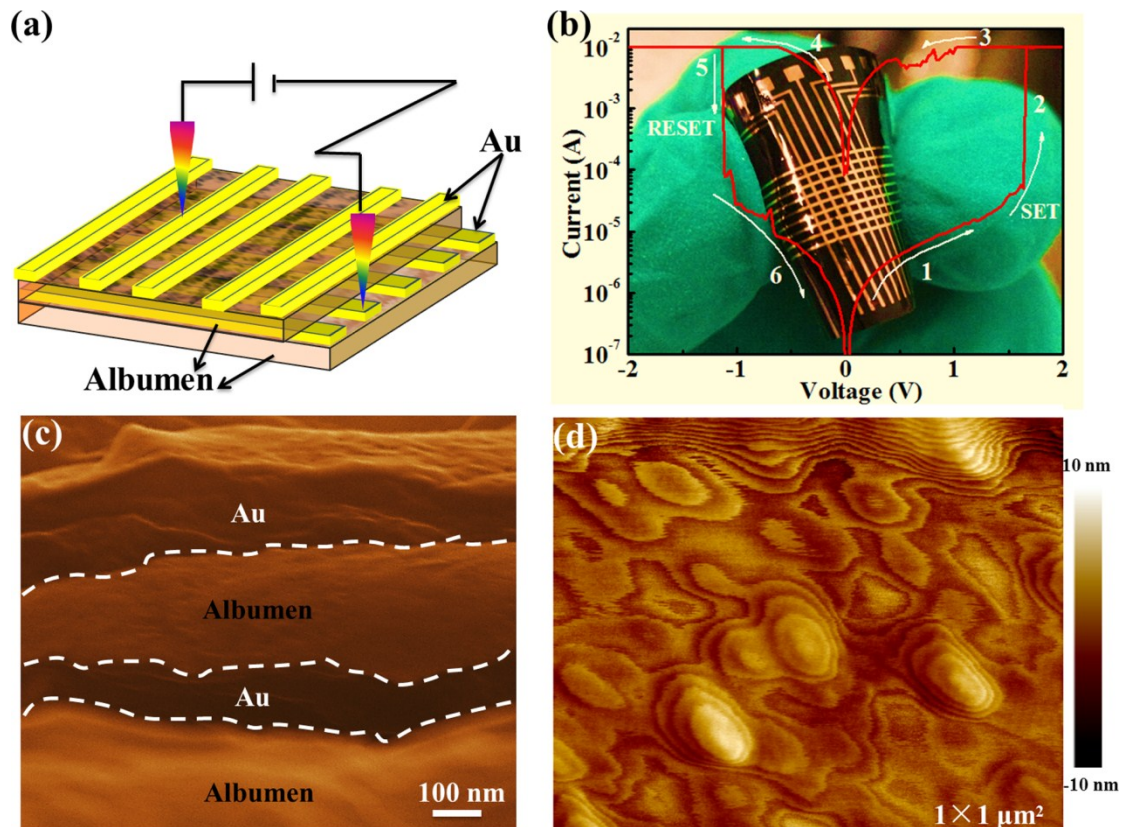


**Fig. S3** Bipolar resistive switching memory behavior and morphology of the device with (a) Albumen|Au|Albumen|Au structure. a. Schematic of the Au|Albumen|Au arrays in flexible albumen substrate. (b) Current-voltage hysteresis for the Au|Albumen|Au memory arrays, and its image is shown in the inset. (c) Cross-section of field emission scanning electron microscope (FE-SEM) image for the Albumen|Au|Albumen|Au memory cell, the egg albumen switching layer is about 100~200 nm. (d) Atomic force microscopy (AFM) image of an albumen film with an area of  $1 \times 1 \mu\text{m}^2$ .

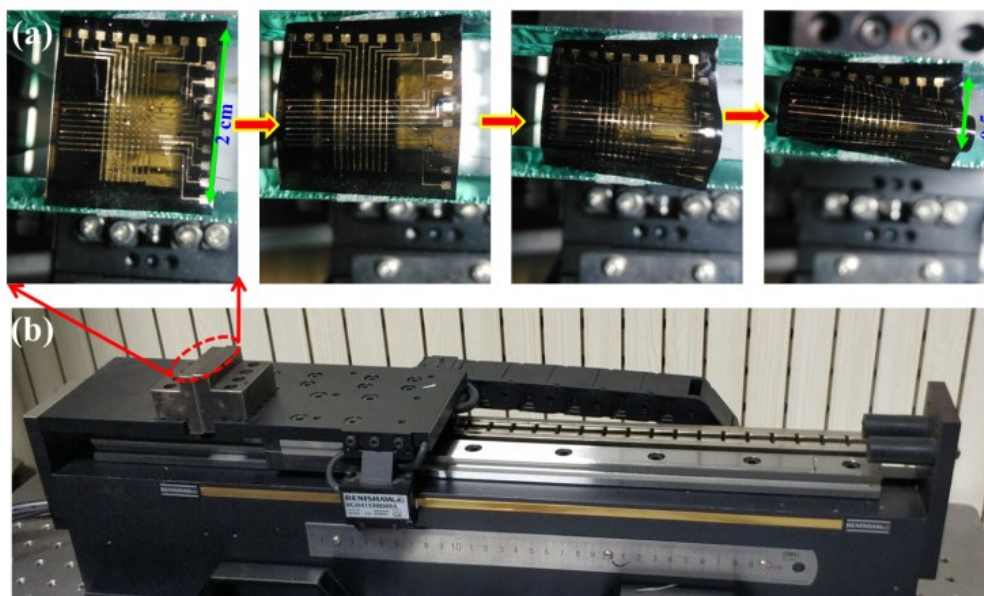


**Fig. S4** (a) The initial distance is 2 cm, which is the flat size of memristor, the final distance is 0.5 cm. The flexibility-base RS behavior can be further investigated after periodic operations. (b) Optic image of line motor system.

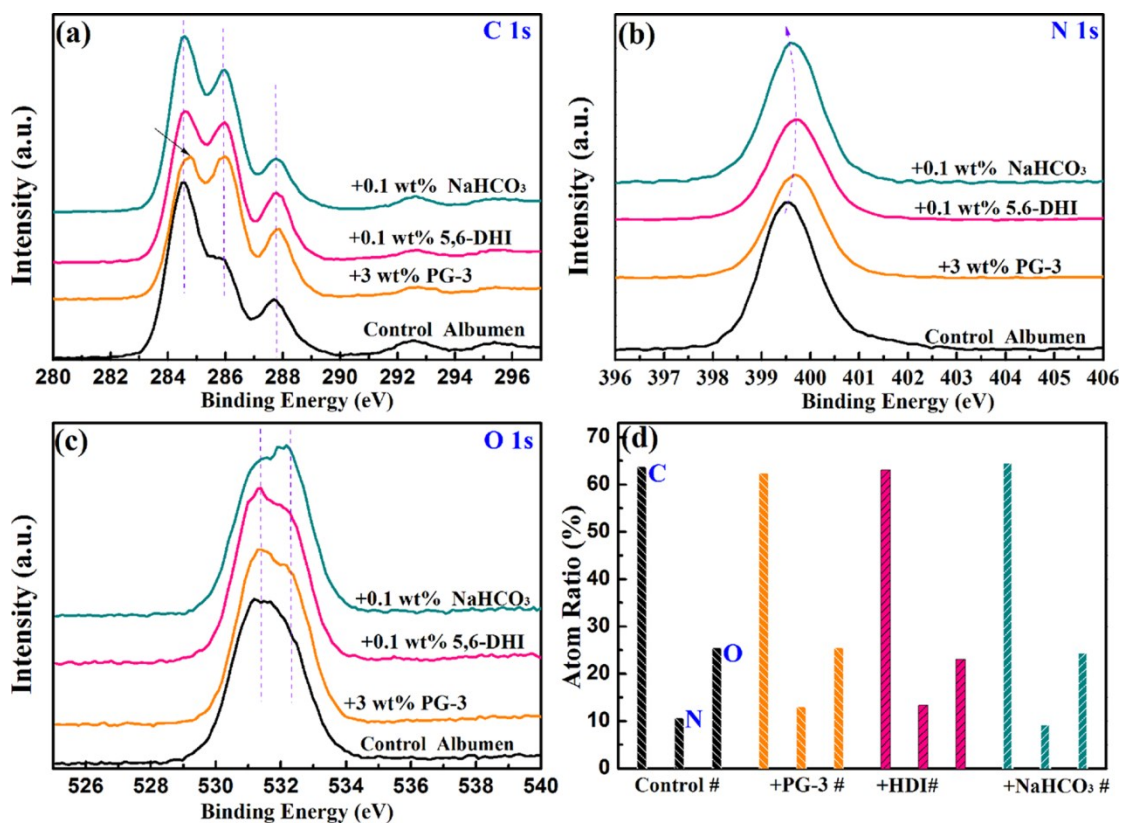


**Fig. S5** X-ray photoelectron spectroscopy (XPS) spectrum of the albumen-based samples. (a) XPS spectrum of the core level of C 1s showing a “blue” shift when adding the 3 wt% Pg-3, but the shift effect is eliminated by adding 0.1 wt% 5,6-DHI and 0.1 wt% NaHCO<sub>3</sub> into the control albumen precursor. (b) XPS spectrum of the core level of N 1s exhibits a “blue shift” and then “red shift” for the studied albumen samples. (c) XPS spectrum of core level of O 1s. The width binding energy of O 1s illustrates that there are a variety of O-based chemical bands in these albumen samples. (d) Atom ratio of C, N and O of albumen control sample, with the 0.1 wt% 5, 6-DHI and 0.1 wt% NaHCO<sub>3</sub>. The binding energy of C 1s and N 1s showing “blue shift” and then “red shift” indicates there are a series of chemical reactions occur when adding the 0.1 wt% 5, 6-DHI and 0.1 wt% NaHCO<sub>3</sub> into the control albumen precursor.

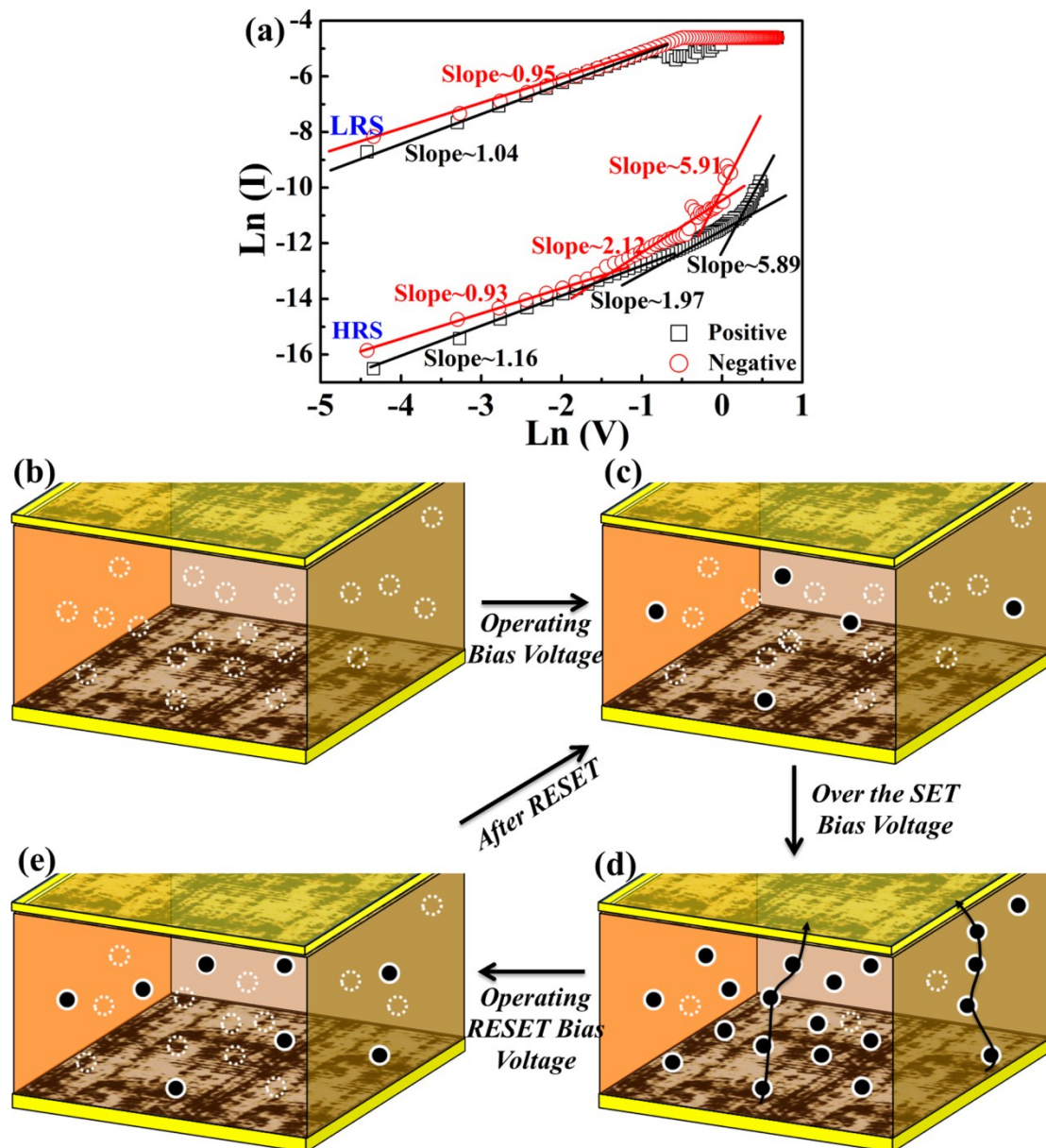


**Fig. S6** Defect site-based physical models for the resistive switching memory of Au|Albumen|Au memory cell. (a) Current-voltage fitted by space charge limited current mechanism. It indicates that the traps such as ions sites fixed by protein network dominate the electron storage and release. (b) Initial state of the albumen active film with trap sites. (c) Injection electrons are trapped by the trap sites when operating bias voltage. (d) Formation of a conductive path between electrodes is triggered by an over set bias voltage leading to the albumen active films switching from HRS to LRS. (e) Rupture of the conductive paths when operation a reset bias voltage.

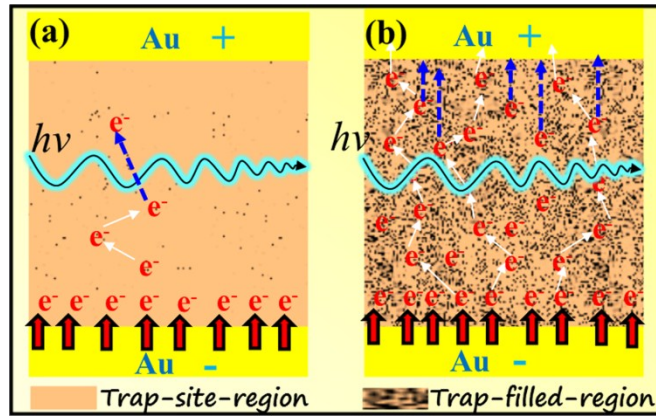


**Fig. S7** Schematic of the influence of light on HRS and LRS. (a) Traps are gradually filled by the injected charges in HRS. The de-trapping and hopping are occurred after operating light illumination, but the contribution is low because of the low concentration of filled trap sites. (b) Nearly all of traps are filled by the injected charges, and a large number of the de-trapping and hopping charges are aroused by the light illumination.

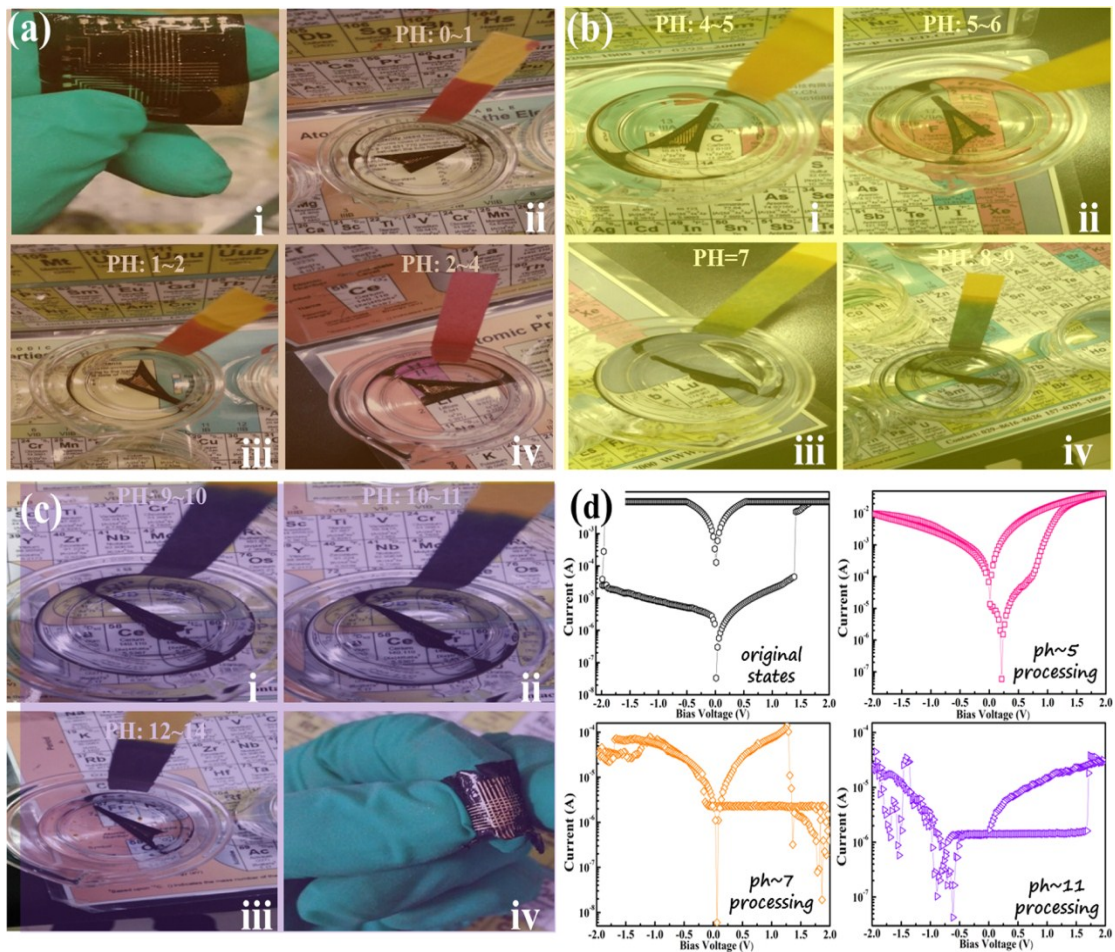


**Fig. S8** The endurance of whole PH range for the RS memory behaviors. (a) The origin egg albumen memristor arrays and being inserted into the HCl solution from the PH 0 to 4. (b) The memristor inserted into HCl and NaOH solution from the PH 4 to 9. (c) The memristor inserted into NaOH solution from the PH 9 to 14. The duration for inserting per PH value is 10 minutes. (d) The RS behaviors for the control memristor arrays, devices dipped in solution with PH~5, ~7 and ~11 , respectively.

Table S1: Storage devices based biomaterials, including the silk protein, DNA, RNA, virus and egg albumen

Materials	Structures	Ratio	Work-	Retention(s)	Functions	Ref.
Silk fibroin	Ag Silk-Fibroin Au	$10^5$	$\pm 1V$	$10^4$	Storage	S-1
DNA	Au CuO-DNA Au Si	$\sim 50$	$\pm 3V$	$10^3$	Storage	S-2
RNA	QD-STV RNA Au	100	$\pm 2V$	$10^6$	Storage	S-3
Virus	Al Virus Al	$10^3$	$\pm 6V$	$10^3$	Storage	S-4
Silk Protein	Mg Silk-Protein Mg	$10^3$	$\pm 2V$	$10^4$	Storage	S-5
Pure-Egg Albumen	Ag Albumen ITO	$10^2$	$\pm 6V$	$10^3$	Storage	Our Previous Work S-6
Fe-doped-Egg	Al/Al <sub>2</sub> O <sub>3</sub> /Albumen: Fe/Al	$10^2$	$\pm 5V$	$10^3$	Storage	S-7
Heated-Egg Albumen	Al Albumen ITO	$10^3$	$\pm 4V$	$10^4$	Storage	S-8
H <sub>2</sub> O <sub>2</sub> -Egg Albumen	Ag Albumen ITO	$10^4$	$\pm 6V$	$10^4$	Storage	Our Previous Work S-6
<b>DHI-Egg Albumen</b>	<b>Au Albumen Au</b>	<b><math>10^4</math></b>	<b><math>\pm 2V</math></b>	<b><math>10^4</math></b>	<b>Memory Logics &amp; Storage</b>	<b>This work</b>

## References:

- S-1 H. Wang, B. Zhu, H. Wang, X. Ma, Y. Hao and X. Chen, *Small*, 2016, **12**, 3360–3365.
- S-2 B. Sun, L. Wei, H. Li, X. Jia, J. Wu and P. Chen, *J. Mater. Chem. C*. 2015, **3**, 12149–12155.
- S-3 T. Lee, A.K. Yagati, F. Pi, A. Sharma, J.W. Choi and P. Guo, *ACS Nano*, 2015, **9**, 6675–6682.
- S-4 R. J. Tseng, C. Tsai, L. Ma, J. Ouyang, C.S. Ozkan and Y. Yang, *Nat. Nanotechnol.* 2006, **1**, 72–77.
- S-5 H. Wang, B. Zhu, X. Ma, Y. Hao and X. Chen, *Small*, 2016, **12**, 2715-2719.
- S-6 G. D. Zhou, Y. Yao, Z. Lu, X. Yang, J. Han, G. Wang, X. Rao, P. Li, Q. Liu and Q. L. Song, *Nanotechnology*, 2017, **28**, 425202.
- S-7 C. C. Lin, C. C. Chung, K. J. Hou and T. L. Tseng, *5th Int. Symp. on. IEEE*, **2016**, 1–2.
- S-8 Y. C. Chen, H. C. Yu, C. Y. Huang, W. L. Chung, S. L. Wu and Y. K. Su, *Sci. Rep.* 2015, **5**, 10022.